

Steric and Electronic Effects of Metal-Containing Substituents in Fischer Carbene Complexes of Chromium

Daniela I. Bezuidenhout, Elisia van der Watt, David C. Liles, Marilé Landman, and Simon Lotz*

Department of Chemistry, University of Pretoria, Pretoria 0002, South Africa

Received February 25, 2008

The Fischer carbene complexes of chromium pentacarbonyl with one or two different metal-containing substituents were synthesized and studied in solution and in the solid state. The dimetallic complexes $[\text{Cr}(\text{CO})_5\{\text{C}(\text{OTiCp}_2\text{Cl})(2\text{-BT})\}]$ (**2**) (BT = benzo[*b*]thienyl) and $[\text{Cr}(\text{CO})_5\{\text{C}(\text{OEt})(\eta^6\text{-2-BT})\text{Cr}(\text{CO})_3\}]$ (**3**) and trimetallic complexes $[\text{Cr}(\text{CO})_5\{\text{C}(\text{OTiCp}_2\text{Cl})(\eta^6\text{-2-BT})\text{Cr}(\text{CO})_3\}]$ (**4**) and $[\text{Cr}(\text{CO})_5\{\text{C}(\text{OTiCp}_2\text{Cl})\text{Fc}\}]$ (**5**) (Fc = ferrocenyl) were prepared and systematically studied with respect to the reference complex $[\text{Cr}(\text{CO})_5\{\text{C}(\text{OEt})(2\text{-BT})\}]$ (**1**) for the importance of the metal substituents in influencing carbene ligand reactivity. It was clear from the crystal structure determination of **4** that most of the unoccupied space was found around the benzo[*b*]thienyl substituent. Hence, it was also possible to synthesize the analogous more crowded trimetallic carbene complex **5** containing an electron-donating ferrocenyl instead of the $[\text{Cr}(\eta^6\text{-2-BT})(\text{CO})_3]$ substituent. Dilithiated ferrocene reacts with 2 equiv of chromium hexacarbonyl, which after alkylation with Et_3OBF_4 affords the ferrocene-1,1'-diyl-bridged biscarbene $[(\text{Cr}(\text{CO})_5)_2\{\mu_2\text{-C}_2(\text{OEt})_2\text{Fe}(\text{C}_5\text{H}_4)_2\text{-C,C'}\}]$ (**7**), while metalation with TiCp_2Cl_2 resulted in the formation of the novel ferrocene-titanocene-bridged biscarbene complex $[(\text{Cr}(\text{CO})_5)_2\{\mu_2\text{-C}_2(\text{O}_2\text{TiCp}_2\text{-O,O}')(\text{Fe}(\text{C}_5\text{H}_4)_2\text{-C,C'})\}]$ (**6**).

Introduction

In recent years, the incorporation of different transition metal fragments in complexes has been widely investigated to study the role of different metal fragments on the reactivity of ligands and the chemistry of the complexes.¹ When applied in the area of Fischer carbene complexes of the type $[\text{M}(\text{CO})_5\{\text{C}(\text{OR}')\text{R}\}]$, either the carbene properties have been modified by introducing metal-containing substituents to further activate the carbene carbon² or the carbene ligand is used as a connector to bridge the other transition metals.³ The introduction of a metal fragment to the carbene oxygen offers the possibility to tune the carbene reactivity by the electronic and steric properties of this second metal fragment.⁴ Recently Raubenheimer and co-workers used

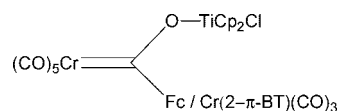


Figure 1. Carbene cluster complexes.

metal carbene anions as bidentate ligands in preparing mixed valence multinuclear complexes.⁵ As far as could be ascertained, no carbene complex has been reported with three different transition metal substituents that are all in electronic contact with the carbene carbon atom, a class of compounds we call carbene cluster compounds. Thus, for this study, carbene complexes of chromium with carbonyl ligands were chosen as being representative of a class of Fischer carbene complexes that exhibit high stability. The carbene substituents selected consisted of titanocene chloride as a titanoxo group and a benzo[*b*]thienyl ring π -coordinated to chromium tricarbonyl or a ferrocenyl substituent (Figure 1), known as an internal electron carrier in conjugated bimetallic carbene complexes.⁶ The procedure for the synthesis of titanoxycarbene complexes in bimetallic complexes has been reviewed.⁴ The objective was not only to synthesize trimetallic carbene complexes but also to systematically study the electronic and steric effects of the different metal-containing substituents by introducing these fragments in a stepwise manner. The structural features and their relevance to bonding in the carbene cluster compounds are discussed and represent indicators of possible reactivity sites in multimetal carbene assemblies. The role of the metal fragments in stabilizing the carbene carbon atom was studied in solution by NMR and in the solid state by X-ray structure determinations.

(5) Raubenheimer, H. G.; du Toit, A.; du Toit, M.; Jin, A.; van Niekerk, I.; Cronje, S.; Esterhuysen, C.; Crouch, A. M. *Dalton Trans.* **2004**, 1173.

(6) Sierra, M. A.; Gómez-Gallego, M.; Martínez-Álvarez, R. *Chem. – Eur. J.* **2007**, 736.

* To whom correspondence should be addressed. E-mail: simon.lotz@up.ac.za. Tel: +27 12 420 2800. Fax: +27 12 420 4687.

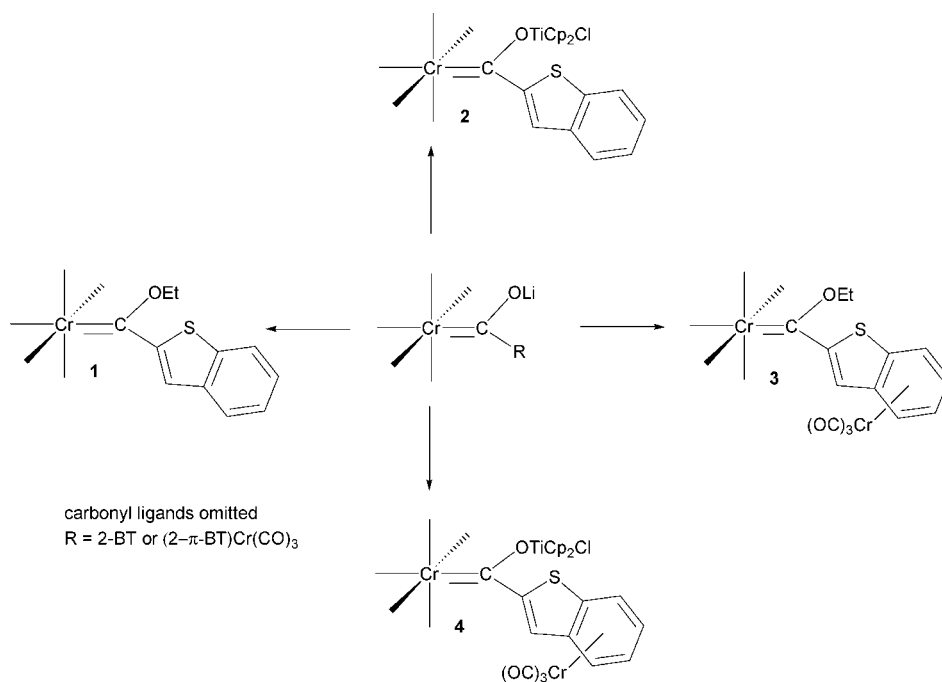
(1) (a) Lotz, S.; van Rooyen, P. H.; Meyer, R. *Adv. Organomet. Chem.* **1995**, 37, 219. (b) Bunz, U. H. F. *Angew. Chem., Int. Ed. Engl.* **1996**, 35, 969. (c) Beck, W.; Niemer, M.; Wieser, M. *Angew. Chem., Int. Ed. Engl.* **1993**, 32, 923. (d) Lang, H. *Angew. Chem., Int. Ed. Engl.* **1994**, 33, 547. (e) Paul, F.; Lapinte, C. *Coord. Chem. Rev.* **1998**, 178–180, 431.

(2) (a) Sierra, M. A. *Chem. Rev.* **2000**, 100, 3591, and references therein. (b) Fuss, B.; Dede, M.; Weibert, B.; Fischer, H. *Organometallics* **2002**, 21, 4425. (c) Crause, C.; Görls, H.; Lotz, S. *Dalton Trans.* **2005**, 1649. (d) Moretó, J. M.; Ricart, S.; Dözt, K. H.; Molins, E. *Organometallics* **2001**, 20, 62.

(3) (a) Bartik, T.; Weng, W.; Ramsden, J. A.; Szafert, S.; Fallon, S. B.; Arif, A. M.; Gladysz, J. A. *J. Am. Chem. Soc.* **1998**, 120, 11071. (b) Weng, W.; Ramsden, J. A.; Arif, A. M.; Gladysz, J. A. *J. Am. Chem. Soc.* **1993**, 115, 3824. (c) Weng, W.; Arif, A. M.; Gladysz, J. A. *Angew. Chem., Int. Ed. Engl.* **1993**, 32, 891. (d) Fischer, E. O.; Röhl, W.; Huy, N. H. T.; Ackermann, K. *Chem. Ber.* **1982**, 115, 2951. (e) Hartbaum, C.; Roth, G.; Fischer, H. *Chem. Ber./Recl.* **1997**, 130, 479. (f) Hartbaum, C.; Mauz, E.; Roth, G.; Weissenbach, K.; Fischer, H. *Organometallics* **1999**, 18, 2619. (g) Terblans, Y. M.; Roos, H. M.; Lotz, S. *J. Organomet. Chem.* **1998**, 566, 133. (h) Landman, M.; Görls, H.; Lotz, S. *Eur. J. Inorg. Chem.* **2001**, 233. (i) Landman, M.; Görls, H.; Lotz, S. *J. Organomet. Chem.* **2001**, 617–618, 280.

(4) Barluenga, J.; Fañanás, F. J. *Tetrahedron* **2000**, 56, 4597, and references therein.

Scheme 1



Results and Discussion

Synthesis of 1–7. For Fischer carbene complexes of the type $[M(CO)_5\{C(OR')R\}]$, π -bonded aryl or heteroaryl ligands can be used to establish electronic contact of the R-substituent or the alkoxy R'-substituent with the carbene carbon atom.⁷ Scheme 1 shows the mono- and dimetal-substituted carbene complexes derived from the benzothienyl substituent. Deprotonation of benzo[*b*]thiophene is accomplished by *n*-BuLi in THF at temperatures below 0 °C, typically at –10 °C, and alkylation of the acylmetalate by triethyloxonium tetrafluoroborate afforded $[Cr(CO)_5\{C(OEt)(2-BT)\}]$ (**1**) in high yields. The deprotonation of the benzo[*b*]thienyl ring π -coordinated to $Cr(CO)_3$ is readily achieved at –40 °C with *n*-BuLi and $[Cr(CO)_5\{C(OEt)((\eta^6-2-BT)Cr(CO)_3)\}]$ (**3**) was obtained in a high yield after alkylation with the oxonium salt. Although the $Cr(CO)_3$ fragment is bonded to the benzene ring in $[Cr(\eta^6-2-BT)(CO)_3]$, deprotonation occurs at the 2-position of the thiophene ring.⁸ It was decided to employ benzo[*b*]thiophene (BTH) as carbene substituent after preliminary experiments with lithiated $[Cr(\eta^5-2\text{-thiophene})(CO)_3]$, and subsequent metalation with titanocene dichloride did not generate the desired trimetallic carbene complexes. Bimetallic titanoxycarbene complexes have been widely studied as a way to use the electron-deficient Lewis acid properties of the titanium to increase the electrophilicity of the carbene carbon atom. This was demonstrated by successfully reacting the titanoxycarbene complex of $[Mn(Cp)(CO)_2\{C(OTiCp_2Cl)R\}]$ in benzannulation reactions, whereas the corresponding alkoxy carbene complexes failed to react.⁹ The most direct and high-yielding method of synthesis is the Fischer route of reacting metal carbonyls with $Ti(NMe_2)_4$.¹⁰ In the context of this work the resulting acylchromate was reacted with titanocene dichloride

to afford $[Cr(CO)_5\{C(OTiCp_2Cl)(2-BT)\}]$ (**2**) in high yields.¹¹ In the preparation of the novel trimetallic carbene complex $[Cr(CO)_5\{C(OTiCp_2Cl)((\eta^6-2-BT)Cr(CO)_3)\}]$ (**4**), lithiation of $[Cr(\eta^6-2-BT)(CO)_3]$ and subsequent reaction with $[Cr(CO)_6]$ was followed by the reaction of the metalate with titanocene dichloride. The relative stability of the complexes in deuterated chloroform was qualitatively assessed and found to decrease in the order **1** > **3** > **4**. Complex **1** is stable in the solid state, whereas **2** and **3** will decompose slowly in solution after a few hours. The instability of **2** is ascribed to the presence of a highly activated chloro ligand after titanoxo formation.¹² Complex **3** is less stable in solution, and loss of the $Cr(CO)_3$ fragment regenerates **1**. The large instability of complex **4** is the result of both these factors. A ¹H NMR spectrum of **4** was not possible in CDCl₃ due to decomposition in solution.

The $[Cr(\eta^6-2-BT)(CO)_3]$ substituent has the π -bonded chromium tricarbonyl fragment coordinated to the ring furthest away from the carbene carbon atom, leaving an unoccupied space directly beneath the thiophene bonded to the carbene carbon atom. This prompted the investigation into the possibility of replacing the benzo[*b*]thiophene fragment by a more compact redox-active ferrocenyl substituent in order to increase the electronic communication between the π -bonded transition metal and the carbene carbon atom (Scheme 2). Monolithiation of ferrocene is best achieved by reaction of ferrocenyl bromide with *n*-BuLi in diethyl ether at –78 °C.¹³ Lithiation of ferrocene in this case was carried out in hexane with 1 equiv of TMEDA at a temperature of 45 °C, yielding both mono- and dilithiated ferrocene. After reacting with $Cr(CO)_6$, the metalate was quenched with titanocene dichloride to yield the trimetallic carbene complex $[Cr(CO)_5\{C(OTiCp_2Cl)Fc\}]$ (**5**) as well as the biscarbene complex containing a bridging bisoxo titanocene and a bridging ferrocen-1,1'-diyl substituent, $[(Cr(CO)_5)_2\{\mu_2-C_2(O_2TiCp_2-O,O')(Fe(C_5H_4)_2-C,C')\}]$ (**6**). The novel complex

(7) (a) Fischer, E. O.; Gammel, F. J.; Neugebauer, D. *Chem. Ber.* **1980**, *113*, 1010. (b) Behrendt, U.; Pfeifer, R.-M.; Warchow, R.; Butenschön, H. *New J. Chem.* **1999**, *23*, 891. (c) Terblans, Y. M.; Lotz, S. *J. Chem. Soc., Dalton Trans.* **1997**, 2177.

(8) du Toit, A.; Landman, M.; Lotz, S. *J. Chem. Soc., Dalton Trans.* **1997**, 2955.

(9) Balzer, B. L.; Cazanoue, M.; Sabat, M.; Finn, M. G. *Organometallics* **1992**, *11*, 1759.

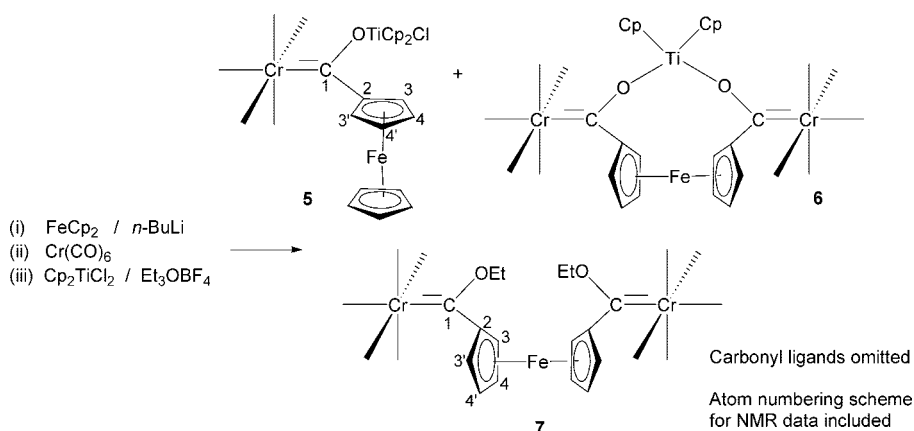
(10) (a) Petz, W. *J. Organomet. Chem.* **1974**, *72*, 369. (b) Pebler, J.; Petz, W. *Z. Naturforsch. B* **1974**, *29*, 658.

(11) (a) Fischer, E. O.; Fontana, S. *J. Organomet. Chem.* **1972**, *40*, 159. (b) Anslyn, E. V.; Santarsiero, B. D.; Grubbs, R. H. *Organometallics* **1988**, *7*, 2137.

(12) Landman, M.; Waldbach, T.; Görls, H.; Lotz, S. *J. Organomet. Chem.* **2003**, *678*, 5.

(13) Fish, R. W.; Rosenblum, M. *J. Org. Chem.* **1965**, *30*, 1253.

Scheme 2



6 is remarkable in that it displays a bimetallic ring bridging the two carbene carbons. In order for comparison with the bisoxo titanocene-bridged biscarbene complex, the dilithiation of ferrocene was repeated, and metalation followed by alkylation with Et_3OBF_4 afforded complex **7**, $[(\text{Cr(CO)}_5)_2\{\mu_2\text{-C}_2(\text{OEt})_2\text{Fe}(\text{C}_5\text{H}_4)_2\text{-C,C'}\}]$, in high yield. Although the monomer $[\text{Cr(CO)}_5\{\text{C}(\text{OEt})\text{Fc}\}]$ is known,¹⁴ the bisethoxy ferrocenyl-bridged biscarbene (**7**) has not been synthesized before.

Unexpectedly, these complexes proved more stable than the trimetallic carbene complex **4**. This could be ascribed to the absence of a displaceable Cr(CO)_3 from BT in the cluster carbene complex, the greater electron-donating character of the ferrocenyl substituent as compared to the $\text{Cr}(\eta^6\text{-2-BT})(\text{CO})_3$ substituent, and the prediction that a ferrocenyl group would not greatly increase the steric crowding around the carbene carbon atom. When comparing complexes **5** and **6**, the absence of an activated chloro ligand on the titanium atom of **6** accounts for its greater stability. It is known that the reaction of a metal acylate with titanocene dichloride by displacement of one of the chloro ligands results in the activation of the remaining chloro ligand and can lead to the formation of two chromium carbene acylates being bridged by a titanocene fragment.^{10b} For the BT- or $[\text{Cr}(\eta^6\text{-BT})(\text{CO})_3]$ -substituted carbene complexes **2** and **4**, it was expected that the remaining chloro ligand on the TiCp_2Cl substituent could be replaced by the acylate of a second carbene; however no biscarbene complexes with bridging bisoxo titanocene substituents could be isolated.

Spectroscopic Characterization of Complexes in Solution.

The signals in the ^1H NMR spectrum of uncoordinated benzo[*b*]thiophene have been resolved, and a full iterative analysis was carried out.¹⁵ Chemical shifts (δ) in ppm measured in CDCl_3 for BTH are as follows: ^1H NMR H2 7.43, H3 7.41, H4 7.92, H5 7.48, H6 7.45, H7 7.98 and ^{13}C NMR C2 121.1, C3 123.7, C4 123.5, C5 124.0, C6 124.1, C7 122.3, C8, C9 139.5, 134 (assignment shown in Figure 2). A 2D HETCOR experiment was used to correctly match H3, H4–H7 with C3, C4–C7. It was not possible to obtain a useful ^{13}C NMR spectrum for **4** due to poor solubility in C_6D_6 and decomposition in CDCl_3 .

Since H3 is the position closest to the site of coordination of the carbene carbon atom, the chemical shift of this proton is influenced most and is a sensitive probe for electronic ring substituent involvement with the electrophilic carbene carbon

atom. Significant downfield shifts of H3 were observed for **1–4** compared to free BTH. The ^1H and ^{13}C NMR data indicated that the benzene resonances are little affected compared to the thienyl proton chemical shifts in **1**, **3**, and **4**. The benzene resonances are shifted upfield in **3** compared to **1** because of coordination to the Cr(CO)_3 fragment. Small upfield shifts in the resonances of the following pairs of complexes, **1** \rightarrow **2** (0.07 ppm) and **3** \rightarrow **4** (0.18 ppm), are observed for the H3 chemical shift values in the ^1H NMR spectra. This is ascribed to the ionic character of the Ti–O bond (**2**, **4**), leading to increased electron density on the oxygen atom, resulting in greater interaction with the carbene carbon atom and less involvement of the BT substituent. Upfield shifts of approximately 0.5 ppm are also observed in the H3 resonances of the following pairs of complexes: **1** \rightarrow **3** and **2** \rightarrow **4**. The corresponding change in structure is $\text{BT} \rightarrow [\text{Cr}(\eta^6\text{-2-BT})(\text{CO})_3]$. In this case, coordination of the Cr(CO)_3 fragment to BT retains more electron density on the rings. To conclude, Figure 3 summarizes the role of metal fragments on electron flow in **4**.

The ^1H NMR spectra of the three ferrocenyl-substituted complexes **5–7** show a downfield shift for the cyclopentadienyl resonances of the ferrocenyl substituent, similar to that of the H3 of the thienyl ring of **1–4**, relative to the Cp resonance of 4.19 ppm for ferrocene. The chemical shifts of both the α - and the β -protons of the attached FeCp ring of **5** and **6** are very

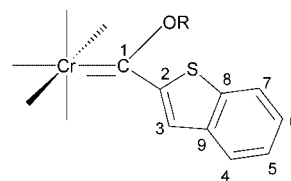
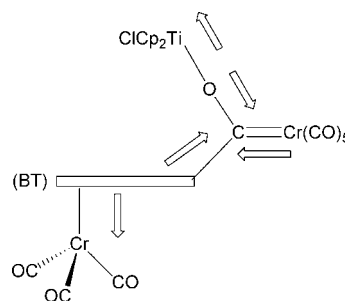


Figure 2. Atom-numbering scheme used for the NMR spectral data.

Figure 3. Role of metal fragments on electron flow in the carbene complex **4**.

(14) Lopez-Cortes, J. G.; de la Cruz, L. F. C.; Ortega-Alfaro, M. C.; Toscano, R. A.; Alvarez-Toledano, C.; Rudler, H. J. *Organomet. Chem.* **2005**, 690, 2229.

(15) (a) Bartle, K. D.; Matthews, R. S.; Jones, D. W. *Tetrahedron* **1971**, 27, 5177. (b) Clark, P. D.; Ewing, D. F.; Scowston, R. M. *Org. Magn. Reson.* **1976**, 8, 252.

similar and display similar downfield shifts compared to other substituted ferrocenes with an electron-withdrawing group, such as $\text{FeCp}(\text{C}_5\text{H}_4(\text{C}(\text{O})\text{OMe}))$ (4.80 H3, H3'; 4.39 H4, H4'; 4.20 Cp).¹⁶ The titanium Cp rings in **2** rotate freely in solution, as is evident from a single peak for the Cp protons as well as carbon atoms in the NMR spectra, while the ^1H NMR spectrum of **4** and the ^{13}C NMR spectrum of **5** show two separate signals. In complex **4** the pyramidal Cp_2Ti group is prochiral, and the π -bonded $\text{Cr}(\text{CO})_3$ group and S atom present in the other carbene substituent exclude the presence of a plane of symmetry that could bisect the Cp–Ti–Cp angle, thus making these two Cp ligands of the Ti group in **4** electronically inequivalent. In complex **5**, this observation is ascribed to restricted rotation of the $\text{C}_{\text{carbene}}\text{--C}_{\text{ferrocenyl}}$ bond caused by the proximity of the bulky metal substituents. The replacement of $\text{Cr}(\eta^6\text{-2-BT})(\text{CO})_3$ with a Fc fragment resulted in a signal of 306 ppm for C1 of **5**, 19 ppm upfield of the C1 resonance for **2**. By contrast, the carbene carbon atom for the biscarbene dimer **6** resonates at 313 ppm. In complex **7** downfield shifts of the $\text{Fe}\text{--C}_5\text{H}_4$ proton resonances are observed compared to **5** and **6**, while upfield shifts of the --OEt protons are observed compared to **1** and **3**. This would support a greater degree of electron donation from the ferrocenyl substituent. The electrophilic carbene carbon atom of **7** is stabilized to such an extent that it shows a ^{13}C NMR resonance at 306 ppm, considerably more upfield than its titanoxo analogue **6**.

The infrared spectra of complexes **1** and **5–7** clearly displayed the expected band pattern associated with the carbonyl stretches of a $\text{Cr}(\text{CO})_5(\text{carbene})$ system.¹⁷ In the case of **2**, the IR spectrum was measured in hexane and shows the lifting of the degeneracy of the E-band that appears as two separate signals. In **3** and **4** some overlapping of the signals associated with the $\text{Cr}(\text{CO})_5$ and $\text{Cr}(\text{CO})_3$ fragment vibration frequencies in the carbonyl region of the spectra complicated assignments.

Crystal and Molecular Structures of the Complexes 1–7. Final confirmations of the structures of the different complexes were obtained from single-crystal X-ray diffraction studies. The complexes crystallized from a dichloromethane/hexane (1:1) solution by layering of the solvents, yielding crystals suitable for diffraction studies. Unfortunately, crystals of **2** exhibited somewhat low diffraction quality and yielded a lower precision crystal structure compared to those obtained for the other complexes. ORTEP¹⁸ + POV-Ray¹⁹ drawings of the molecular structures of **1–7**, showing the atom-numbering scheme, are presented in Figures 4–10. Crystal data, refinement parameters, and experimental details are given in the Experimental Section. Selected bond lengths, bond angles, and torsion angles are given in Tables 1 (**1–4**) and 2 (**5–7**). For **1** the atoms of the $\text{C}(\text{OEt})\text{BT}$ ligand (except for four of the five hydrogen atoms of the Et group) together with the Cr and the CO *trans* to the carbene ligand all lie in a mirror plane. In the structures of complexes **4**, **5**, and **7** the thienyl or cyclopentadienyl ring is also approximately coplanar with the carbene moiety (Cr(1), C(6), O(6), C(7)). The angle between the plane of the carbene and that of the five-membered ring is $1.6(3)^\circ$, $3.3(3)^\circ$, and $0.83(6)^\circ$, respectively, and the torsion angles Cr(1)–C(6)–C(7)–C(8) and O(6)–C(6)–C(7)–S(1)/C(11) are all in the range $-1.7(5)^\circ$ to $2.7(6)^\circ$ for the three complexes. However, the resonance stabilization afforded by the carbene

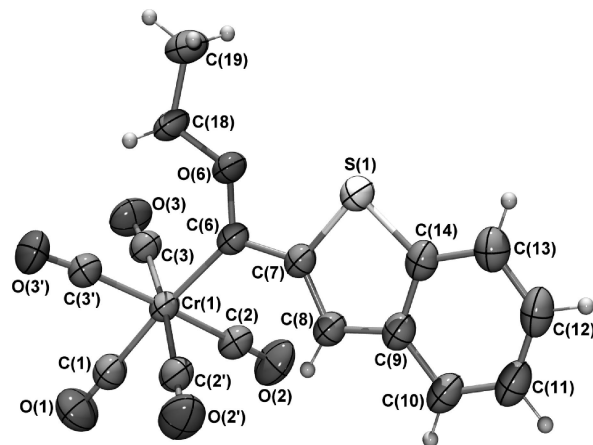


Figure 4. ORTEP + POV-Ray drawing of the molecular structure of **1**. Atomic displacement ellipsoids are shown at the 50% probability level.

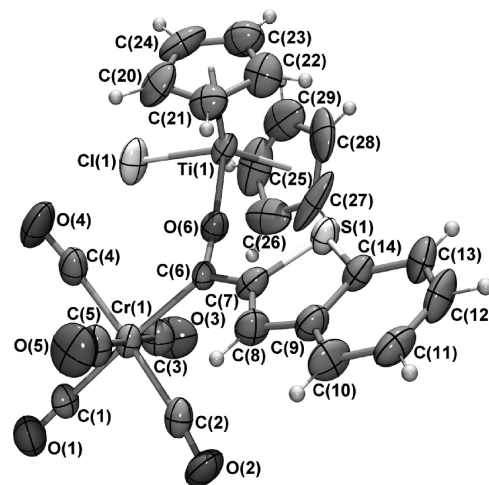


Figure 5. ORTEP + POV-Ray drawing of the molecular structure of **2**. Atomic displacement ellipsoids are shown at the 50% probability level.

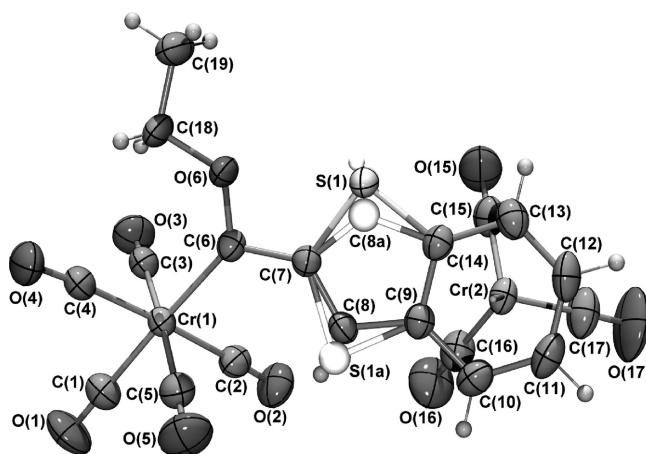


Figure 6. ORTEP + POV-Ray drawing of the molecular structure of **3**. Atomic displacement ellipsoids are shown at the 50% probability level.

moiety being approximately coplanar with the adjacent ring is presumably weak and may easily be overridden by the exigencies of either packing forces, as observed in complexes **2** and **3**, where the angle between the plane of the carbene and that of the thienyl ring is $13.2(5)^\circ$ and $9.60(10)^\circ$, respectively, or the

(16) Pickett, T. E.; Richards, C. J. *Tetrahedron Lett.* **1999**, 40, 5251.

(17) Braterman, P. S. *Metal Carbonyl Spectra*; Academic Press Inc.: London, 1975; p 68.

(18) Farrugia, L. J. *J. Appl. Crystallogr.* **1997**, 30, 565.

(19) The POV-Ray team. *POV-Ray*, 2004. URL: <http://www.povray.org/download/>.

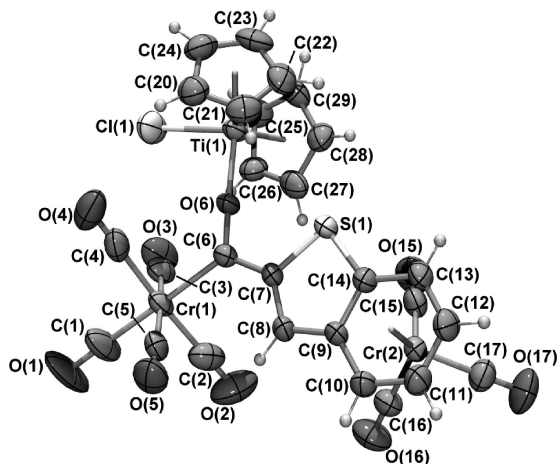


Figure 7. ORTEP + POV-Ray drawing of the molecular structure of **4**. Atomic displacement ellipsoids are shown at the 50% probability level.

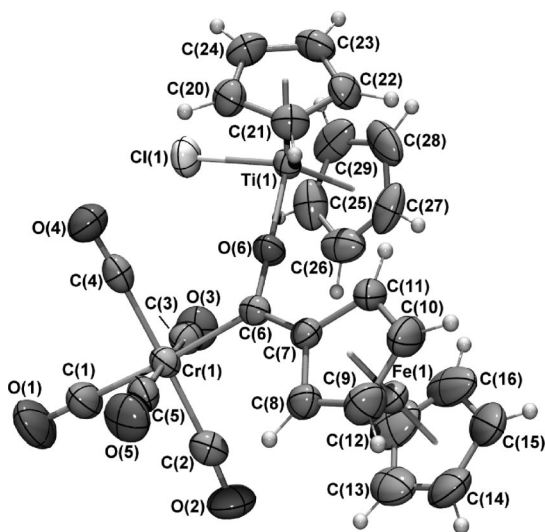


Figure 8. ORTEP + POV-Ray drawing of the molecular structure of **5**. Atomic displacement ellipsoids are shown at the 50% probability level.

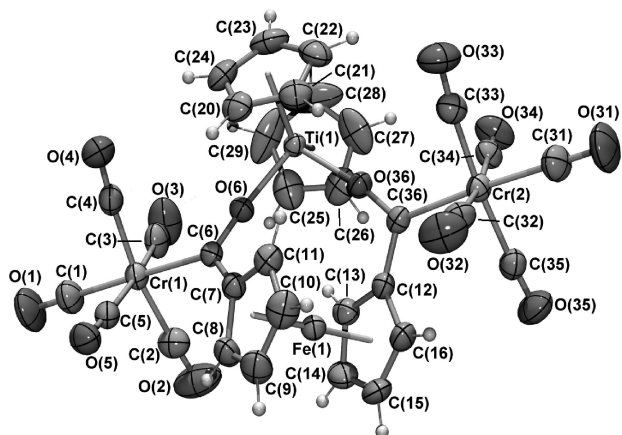


Figure 9. ORTEP + POV-Ray drawing of the molecular structure of **6**. Atomic displacement ellipsoids are shown at the 50% probability level.

steric requirements of the molecule, as observed in **6**, where the corresponding angles are $32.17(10)^\circ$ and $28.78(9)^\circ$. In complexes **1–4** the BT substituent is essentially planar, with

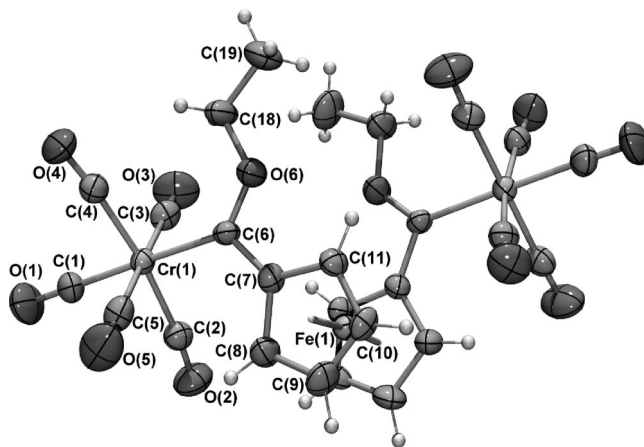


Figure 10. ORTEP + POV-Ray drawing of the molecular structure of **7**. Atomic displacement ellipsoids are shown at the 50% probability level.

the angle between the mean planes of the five- and six-membered rings being 0.0° , $2.5(6)^\circ$, $1.47(14)^\circ$, and $1.8(3)^\circ$ for **1**, **2**, **3**, and **4** respectively. The Ti(1)–O(6/36) bonds in **2**, **4**, **5**, and **6** are significantly longer (1.905(3)–1.9514(15) Å) than those of typical terminal titanium(IV) alkoxides (1.855(2) Å in $\text{TiCp}_2(\text{OEt})\text{Cl}$).²⁰ This is indicative of O(6) \rightarrow C(6) π -donation occurring at the expense of O(6) \rightarrow Ti(1) π -donation and is further supported by the short C(6)–O(6) and C(36)–O(36) bond distances (1.274(2)–1.286(5) Å) that are significantly shorter than the range of 1.305(4)–1.324(3) Å observed for **1**, **3**, **7**, $[\text{Cr}(\text{CO})_5\{\text{C}(\text{OEt})\text{Fc}\}]$,¹⁴ and $[\text{Cr}(\text{CO})_5\{\text{C}(\text{OMe})(\text{C}_5\text{H}_4)\text{-Fe}(\text{C}_5\text{H}_4\text{Br})\}]$.²¹ Erker has also noted that an acyl resonance structure is an important contributor to the bonding of zirconoxy carbene complexes.²² Observing the near linear C(6/36)–O(6/36)–Ti(1) bond angles, in the range $169.76(15)$ – $178.5(3)^\circ$, for **2**, **4**, **5**, and **6**, the acyl character of the carbene–oxygen bond, and the very long titanium–oxygen bond, one can conclude that a significant ionic character is present in the titanium–oxygen bonds, with the electropositive Lewis acid TiCp_2X fragment on the one side of the carbene oxygen atom and an electrophilic carbene carbon on the other side (Figure 11). This manifests in a short C(carbene)–O distance and a long Ti–O distance, the net result of strong competition between these two fragments for electron density. The C(carbene)–C(BT/Fc) distances are similar for all the complexes and fall in the range 1.461(13)–1.483(3) Å. In general in the molecular structures of the BT complexes, the sulfur atom of the thienyl ring is *cis* to the oxygen atom of the ethoxy substituent, indicating either restricted rotation around the C(6)–C(7) bond or a preferred packing order in the solid state. However, in contrast to the structures of **1**, **2**, and **4**, that of **3** exhibits a minor isomeric form with the sulfur atom in the thienyl ring *trans* to the ethoxy substituent in addition to the *cis* major isomer (88%) (Figure 6). The precursor $[\text{Cr}(\eta^6\text{-BT})(\text{CO})_3]$ is presumably formed in a 1:1 mixture of isomers (Figure 12). So for both **3** and **4** in solution a 1:1 mixture of the isomers of the $\text{Cr}(\text{CO})_3$ on one or the other face of the benzene ring (planar chirality)²³ is formed, but with the thienyl S remaining *cis* to the carbene O. Both form crystals that have

(20) Huffman, J. C.; Moloy, K. G.; Marsella, J. A.; Caulton, K. G. *J. Am. Chem. Soc.* **1980**, *102*, 3009.

(21) Hursthouse, M. B.; Hibbs, D. E.; Butler, I. R. Private communication, 2003. Cambridge Structural Database (Allen, F. H. *Acta Crystallogr.* **2002**, B58, 380), CCDC 262965.

(22) Erker, G. *Angew. Chem., Int. Ed. Engl.* **1989**, *28*, 397.

(23) Schlögl, K. *J. Organomet. Chem.* **1986**, *300*, 219.

Table 1. Selected Bond Lengths (Å), Bond Angles (deg), and Torsion Angles (deg) for 1–4

bond lengths	1	2	3	4
Cr(1)–C(6)	2.067(2)	2.104(7)	2.050(2)	2.077(4)
C(6)–O(6)	1.319(3)	1.275(9)	1.324(3)	1.285(5)
C(6)–C(7)	1.462(3)	1.461(13)	1.472(3)	1.463(6)
O(6)–C(18)	1.447(3)		1.453(3)	
O(6)–Ti(1)		1.934(5)		1.925(3)
Cr(1)–C(1)	1.875(3)	1.926(9)	1.884(3)	1.859(6)
Cr(1)–C(2,3,4,5) ^a	1.9044(19)	1.903(10)	1.905(3)	1.898(7)
C(7)–C(8)	1.368(3)	1.362(12)	1.354(4)	1.363(6)
C(8)–C(9)	1.421(4)	1.421(15)	1.439(3)	1.438(6)
C(9)–C(14)	1.399(4)	1.402(11)	1.408(3)	1.414(6)
C(14)–S(1)	1.727(3)	1.734(10)	1.726(2)	1.724(5)
C(7)–S(1)	1.758(3)	1.748(9)	1.763(2)	1.770(4)
bond angles	1	2	3	4
C(1)–Cr(1)–C(6)	175.09(10)	173.9(3)	177.75(10)	178.0(3)
O(6)–C(6)–C(7)	105.2(2)	114.0(6)	104.52(18)	112.7(4)
O(6)–C(6)–Cr(1)	129.94(17)	120.0(6)	130.04(15)	120.9(3)
C(7)–C(6)–Cr(1)	124.89(17)	125.9(5)	125.36(15)	126.4(3)
C(6)–O(6)–C(18)	123.2(2)		124.28(18)	
C(6)–O(6)–Ti(1)		172.1(5)		174.0(3)
C(6)–C(7)–S(1)	119.52(18)	119.8(6)	117.69(15)	119.8(3)
torsion angles	1	2	3	4
C(3)–Cr(1)–C(6)–O(6)	44.16(6)	44.3(6)	50.2(2)	42.1(4)
Cr(1)–C(6)–O(6)–C(18)	0.0		3.5(4)	
O(6)–C(6)–C(7)–S(1)	0.0	–11.2(9)	–8.2(2)	–1.7(5)
Cr(1)–C(6)–C(7)–C(8)	0.0	–14.0(12)	–8.5(4)	1.1(7)
S(1)–C(14)–C(9)–C(10)	180.0	–176.0(7)	–179.87(18)	179.4(4)
C(8)–C(9)–C(14)–C(13)	180.0	–179.7(8)	–177.0(2)	–175.5(4)

^a Averaged value (Cr(1)–C(2,3) for 1).

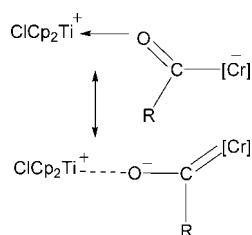


Figure 11. Acyl resonance and ionic O[−]/Ti⁺ interaction for titanoxycarbene complexes.

centrosymmetric space groups, so both isomers are present in the crystals in a 1:1 mixture. However, in **3** the barrier to rotation about the C(6)–C(7) bond is sufficiently small so that a portion of one isomer can rotate to fit the crystal space occupied by the other isomer with the Cr(CO)₃ groups occupying the same positions. In **4** the steric hindrance introduced by the titanoxycarbene substituent prevents such a rotation from occurring. The tripod described by the carbonyl ligands of the Cr(CO)₃ fragment in **3** and **4** adopted a staggered *S*-conformation, which correlates with an electron-withdrawing condensed thiophene ring and supports the electronic conclusions drawn from the NMR spectroscopy.²⁴ Table 3 summarizes the bond distances and bond angles surrounding the carbene carbon atom. The Cr–C(carbene) distances fall in the range 2.050(2)–2.104(7) Å, which are typical for alkoxy carbene complexes of Cr(CO)₃.²⁵

The bond angles around the carbene carbon atom, defined as angles 1–3 in Table 3, depend on the steric requirements of the groups bonded to that carbon atom. Angle 2 (Cr–C–C) remains more or less constant for all seven complexes, as the steric requirements of the thienyl and cyclopentadienyl moieties, with respect to the carbonyl ligands *cis* to the carbene, are

similar. The complexes have a ring C–H *ortho* to the carbene lying staggered with respect to two adjacent carbonyl ligands and in close contact with them, leading to somewhat strained sp² angles in the range 122.9(2)–127.3(3)° for angle 2, compared to the Cr–C–C bond angle of ca. 121° for the sterically undemanding substituted complex [Cr(CO)₅{C(OEt)Me}].²⁶ In contrast, the moiety bonded to the carbene via the oxygen atom results in marked differences in the geometry around the carbene carbon atom. In the complexes with a titanoxycarbene substituent, the nearly linear geometry at oxygen together with the comparatively long Ti–O bonds allows the OTiCp₂X moieties to be accommodated in the complexes with little or no steric strain, allowing angle 1 (Cr–C–O) to adopt unstrained sp² values of ca. 120° (these angles are ca. 3° larger in **6** to accommodate both the –O–Ti–O– and the ferrocene-1,1'-diyl bridges between the two carbene ligands), whereas in the complexes with an ethoxy substituent, the ethoxy group adopts an orientation such that the methylene carbon is in a similar position relative to the second pair of carbonyl ligands *cis* to the carbene as the *ortho* carbon in the thienyl or cyclopentadienyl ring is to the first pair of carbonyls. This agrees with the findings of Sierra that alkoxy-carbenes occur in the *anti* conformation, where the oxygen lone pairs are found *trans* to the M=C bond, even in the case of the titanoxycarbene complexes.²⁷ The presence of two hydrogen atoms bonded to the methylene carbon, together with shorter C–O bond distances compared with the C–C(ring) bond distances, induces even greater strain than induced by the ring C–H, leading to values of ca. 130° for angle 1, similar to the Cr–C–O bond of 132.01° of the sterically unhindered [Cr(CO)₅{C(OEt)Me}].

Experimental Section

General Procedures. All manipulations involving organometallic compounds made use of Schlenk techniques, and operations were

(24) Muetterties, E. L.; Bleeke, J. R.; Wucherer, E. J.; Albright, T. A. *Chem. Rev.* **1982**, 82, 499.

(25) Dötz, K. H.; Fischer, H.; Hofmann, P.; Kreissl, F. R.; Schubert, U.; Weiss, K. *Transition Metal Carbene Complexes*; VCH Verlag Chemie: Weinheim, 1983.

(26) Kruger, C.; Goddard, R.; Claus, K. H. *Z. Naturforsch., B: Chem. Sci.* **1983**, 38, 1431.

(27) Andrada, D. M.; Zoloff Michoff, M. E.; Fernández, I.; Granados, A. M.; Sierra, M. A. *Organometallics* **2007**, 26, 5854.

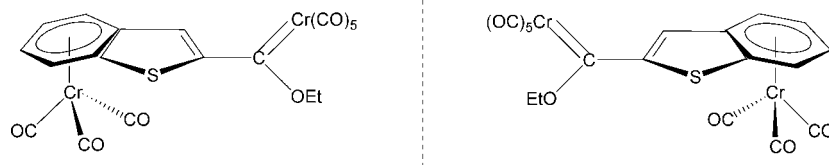
Figure 12. Planar chirality in the $\text{Cr}(\eta^6\text{-BT})(\text{CO})_3$ -carbene complexes.

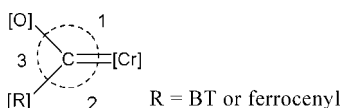
Table 2. Selected Bond Lengths (Å), Bond Angles (deg), and Torsion Angles (deg) for 5–7

bond lengths ^a	5	6	7
Cr(1)–C(6), Cr(2)–C(36)	2.090(4)	2.063(2)	2.077(2)
C(6)–O(6), C(36)–O(36)	1.286(5)	1.276(2)	1.274(2)
C(6)–C(7), C(36)–C(12)	1.472(6)	1.480(3)	1.483(3)
O(6)–C(18)			1.447
O(6)–Ti(1), O(36)–Ti(1)	1.905(3)	1.9507(14)	1.9514(15)
Cr(1)–C(1), Cr(2)–C(31)	1.863(5)	1.882(3)	1.873(3)
Cr(1)–C(2,3,4,5) ^b	1.893(6)	1.892(3)	1.903(3)
bond angles ^a	5	6	7
C(1)–Cr(1)–C(6), C(31)–Cr(2)–C(36)	175.9(2)	177.32(10)	175.84(11)
O(6)–C(6)–C(7), O(36)–C(36)–C(12)	112.9(3)	113.81(18)	113.66(18)
O(6)–C(6)–Cr(1), O(36)–C(36)–Cr(2)	119.7(3)	122.91(15)	123.29(15)
C(7)–C(6)–Cr(1), C(12)–C(36)–Cr(2)	127.3(3)	123.12(14)	122.93(15)
C(6)–O(6)–C(18)			123.1(3)
C(6)–O(6)–Ti(1), C(36)–O(36)–Ti(1)	178.5(3)	169.76(15)	170.10(14)
C(6)–C(7)–C(8), C(36)–C(12)–C(13)	126.2(4)	127.0(2)	126.4(2)
C(6)–C(7)–C(11), C(36)–C(12)–C(16)	127.4(4)	127.2(2)	127.7(2)
torsion angles ^a	5	6	7
C(3)–Cr(1)–C(6)–O(6), C(33)–Cr(2)–C(36)–O(36)	44.1(3)	24.79(19)	30.81(18)
Cr(1)–C(6)–O(6)–C(18)			2.1(9)
O(6)–C(6)–C(7)–C(11), O(36)–C(36)–C(12)–C(13)	–1.0(6)	29.5(3)	25.9(3)
Cr(1)–C(6)–C(7)–C(8), Cr(2)–C(36)–C(12)–C(16)	2.7(6)	34.3(3)	31.0(3)

^a The second designated bond length, bond angle, or torsion angle refers to geometry involving the second Cr carbene moiety in **6**. These values are tabulated in the second column under **6**. ^b Averaged value (Cr(1)–C(2,3,4,5) + Cr(2)–C(32,33,34,35) for **6**).

Table 3. Selected Bond Lengths (Å) and Angles (deg) around the Carbene Carbon in 1–7

angle	1	2	3	4	5	6	7
1	129.9(2)	120.0(6)	130.0(2)	120.9(3)	119.7(3)	122.9(2) 123.3(2)	130.2(2)
2	124.9(2)	125.9(5)	124.4(2)	126.4(3)	127.3(3)	123.1(1) 122.9(2)	124.6(2)
3	105.2(2)	114.0(6)	104.5(2)	112.7(4)	112.9(3)	113.8(2) 113.7(2)	105.2(3)
bond	1	2	3	4	5	6	7
Cr–C _{carb}	2.067(2)	2.104(7)	2.050(2)	2.077(4)	2.090(4)	2.063(2) 2.077(2)	2.083(3)
C _{carb} –O	1.319(3)	1.275(9)	1.324(3)	1.285(5)	1.286(5)	1.276(2) 1.274(2)	1.305(4)
C _{carb} –C(R)	1.462(3)	1.461(13)	1.472(3)	1.463(6)	1.472(6)	1.480(3) 1.483(3)	1.464(4)



carried out under an inert atmosphere. Hexane, THF, and dichloromethane were dried and deoxygenated by distillation prior to being used. $\text{Cr}(\text{CO})_6$, ferrocene, $n\text{-BuLi}$ (1.6 mol/dm³ solution in hexane), benzo[*b*]thiophene, and titanocene dichloride were used as purchased. Triethyloxonium tetrafluoroborate was prepared according to literature procedures,²⁸ and TMEDA was distilled before use. $[\text{Cr}(\eta^6\text{-2-BT})(\text{CO})_3]$ was prepared from triammine(tricarbonyl)chromium by a modified literature procedure.²⁹ Column chromatography using silica gel 60 (0.0063–0.200 mm) or neutral aluminum oxide as stationary phase was used for all separations, and columns were cooled by circulating ice–water through the column jackets. Melting points were not recorded due to decomposition during heating. NMR spectra were recorded on a Bruker ARX-300 spectrometer and on a AVANCE 500 spectrometer. ¹H NMR spectra were recorded at 300.135 and 500.139 MHz and ¹³C NMR spectra at 75.49 and 125.75 MHz, respectively. The signal

of the deuterated solvent was used as reference, e.g., ¹H CDCl₃ 7.24 ppm and ¹³C CDCl₃ 77.00 ppm. IR spectra were recorded on a Perkin-Elmer Spectrum RXI FT-IR spectrophotometer. All spectra were recorded using either dichloromethane or hexane as solvent. Only the vibration bands in the carbonyl-stretching region (ca. 1600–2200 cm^{–1}) were recorded.

Preparation of (η^6 -Benzo[*b*]thiophene)tricarbonylchromium.³⁰ Triammine(tricarbonyl)chromium (2.00 g, 10.7 mmol) was dissolved in diethyl ether (90 mL). Freshly distilled boron trifluoride diethyl etherate (3.95 mL, 33 mmol) was added to the solution, followed by 2.82 g (21 mmol) of benzo[*b*]thiophene. The reaction mixture was stirred for 12 h. Diethyl ether (100 mL) was added, and the solution was cooled to 0 °C, after which 100 mL of air-free water was added. The mixture was repeatedly extracted with diethyl ether until the extracts were virtually colorless. The ether extracts were combined and dried over anhydrous sodium sulfate. The solvent was removed under

(28) Meerwein, H. *Org. Synth.* **1966**, 46, 113.

(29) Zaiko, E. J.; Lipman, L., Jr.; Moser, G. A.; Rausch, M. D. *J. Organomet. Chem.* **1970**, 23, 185.

(30) (a) Schmidt, S. P.; Nitschke, J.; Troglor, W. C. *Inorg. Synth.* **1989**, 26, 115. (b) Novi, M.; Guanti, G. *J. Heterocycl. Chem.* **1975**, 12, 1055.

reduced pressure. The product was purified with column chromatography, which afforded the starting compounds and the orange product. The crude product was crystallized from dichloromethane and hexane. The orange crystals were washed with hexane and dried under reduced pressure. Yield: 0.97 g (34%).

General Method for the Synthesis of Fischer Carbene Complexes 1–4. The dropwise addition of a 1.6 mol dm⁻³ hexane solution of *n*-BuLi (0.7 mL, 1.1 mmol) to a cooled (−30 °C) THF solution (12 mL) containing benzo[*b*]thiophene (0.14 g, 1 mmol) or (η^6 -benzo[*b*]thiophene)tricarbonylchromium(0) (0.27 g, 1 mmol) afforded a lithiated thienyl species in high yields after 30 min. Addition of chromium hexacarbonyl (0.22 g, 1 mmol) in small portions over 10 min resulted in a gradual change of color from orange to yellow. After stirring for 1 h in the cold, the reaction mixture was warmed to room temperature and stripped of solvent under reduced pressure. The residue was dissolved in dichloromethane, cooled to −30 °C, and carefully treated with triethyloxonium tetrafluoroborate (0.20 g, 1 mmol) or titanocene dichloride (0.25 g, 1 mmol), also dissolved in dichloromethane. After stirring for 1 h and allowing the reaction mixture to warm to room temperature, the dark-colored solution was filtered through silica gel or neutral aluminum oxide and washed through with dichloromethane. The solution was evaporated under reduced pressure to give a dry residue and purified with column chromatography using hexane/dichloromethane (1:1) as eluent.

Preparation of 5–7. Ferrocene (0.18 g, 1 mmol) was dissolved in hexane (20 mL). Then a 1.6 mol dm⁻³ hexane solution of *n*-BuLi (0.7 mL, 1.1 mmol) and TMEDA (0.15 mL, 1 mmol) was mixed and added to the ferrocene. This mixture was stirred while increasing the temperature, until the orange adduct precipitated from the hexane solution. The excess liquid was decanted from the precipitate, and the residue was dissolved in 20 mL of freshly distilled THF. Chromium hexacarbonyl (0.22 g, 1 mmol) was dissolved in THF (10 mL), cooled to −50 °C, and added to the precipitate. After stirring for 1 h in the cold, the reaction mixture was warmed to room temperature and stripped of solvent under reduced pressure. The residue was washed several times with hexane, dissolved in dichloromethane, cooled to −30 °C, and carefully treated with titanocene dichloride (0.25 g, 1 mmol), also dissolved in dichloromethane. After stirring for 1 h and allowing the reaction mixture to warm to room temperature, the red-brown-colored solution was filtered through silica gel with dichloromethane. The solution was dried *in vacuo* and washed with hexane. The resulting dark brown product afforded three bands on purification with column chromatography (eluent: dichloromethane/hexane, 1:1). The first orange band afforded the starting material, ferrocene, yield: 0.05 g (8%). The second dark brown product was identified as **6**, while the third red-brown band yielded **5**.

Complex **7** was prepared by repeating the above procedure, but instead of quenching the reaction with titanocene dichloride, the chromium acylate was alkylated using (0.42 g, 2.2 mmol) triethyloxonium tetrafluoroborate. The orange monomer [Cr(CO)₅{C(OEt)Fc}]¹⁴ was isolated as the band following the unreacted starting material ferrocene on the column, while the third red band afforded **7**.

[Cr(CO)₅{C(OEt)(2-BT)}] (**1**): yield 0.26 g, 68%. NMR (δ /ppm in CDCl₃): ¹H NMR 8.50 (d, 1H, H₃, *J* = 0.8 Hz), 7.80 (ddd, 1H, H₄, *J* = 8.0, 1.8, 0.8 Hz) 7.49 (ddd, 1H, H₅, *J* = 8.0, 1.03 Hz), 7.40 (ddd, 1H, H₆, 7.8, 1.8 Hz), 8.00 (dd, 1H, H₇, *J* = 7.8, 1.03 Hz), 5.25 (q, 2H, CH₂, *J* = 7.0 Hz), 1.72 (t, 3H, CH₃, *J* = 7.0 Hz). ¹³C NMR: 320 (C1), 217 (CO_{cis}), 223 (CO_{trans}), 154 (C2), 142 (C3), 123 (C4), 129 (C5), 125 (C6), 127 (C7), 138.7, 139.2 (C8, C9), 77 (CH₂), 15 (CH₃). IR (ν_{CO} , hexane, cm⁻¹): 2058 m (A₁'), 1984 w (B), 1959 s (A₁'), 1948 vs (E). Anal. Calcd for C₁₆H₁₀SO₆Cr: C, 50.26; H, 2.62. Found: C, 50.47; H 2.71.

[Cr(CO)₅{C(OTiCp₂Cl)(2-BT)}] (**2**): yield 0.27 g, 49%. NMR (δ /ppm in CDCl₃): ¹H NMR 8.43 (s, 1H, H₃), 7.87 (dd, 1H, H₄, *J* = 8.1 Hz) 7.50 (m, 1H, H₅, *J* = 8.1, 1.2 Hz), 7.45 (m, 1H, H₆, 7.1, 1.8 Hz), 8.04 (dd, 1H, H₇, *J* = 7.1, 1.2 Hz), 6.55 (s, 10H, Cp). ¹³C NMR: 325 (C1), 218 (CO_{cis}), 225 (CO_{trans}), 141 (C2), 140 (C3), 123 (C4), 128 (C5), 125 (C6), 127 (C7), 138, 138 (C8, C9), 119 (Cp). IR (ν_{CO} , hexane, cm⁻¹): 2050 m (A₁'), 1987 w (B), 1948 s (A₁'), 1936 vs, 1915s (E). Anal. Calcd for C₂₄H₁₅SClO₆Cr: C, 50.87; H, 2.67. Found: C, 51.09; H 2.79.

[Cr(CO)₅{C(OEt)((η^6 -2-BT)Cr(CO)₃)}] (**3**): yield 0.26 g, 50%. NMR (δ /ppm in CDCl₃): ¹H NMR 8.13 (d, 1H, H₃, *J* = 0.8), 6.07 (dd, 1H, H₄, *J* = 6.8, 0.8 Hz) 5.61 (m, 1H, H₅, *J* = 6.8, 0.9 Hz), 5.26 (m, 1H, H₆, *J* = 6.6 Hz), 6.29 (dd, 1H, H₇, *J* = 6.6, 0.9 Hz), 5.19 (q, 2H, CH₂, *J* = 7.0 Hz), 1.69 (t, 3H, CH₃, *J* = 7.0 Hz). ¹³C NMR: 318 (C1), 231 (Cr(CO)₃), 217 (CO_{cis}), 223 (CO_{trans}), 156 (C2), 138 (C3), 89 (C4), 90 (C5), 92 (C6), 84 (C7), 118, 127 (C8, C9), 77 (CH₂), 15 (CH₃). IR (ν_{CO} , hexane, cm⁻¹): Cr(CO)₅: 2059 m (A₁'), 1989 vw (B), 1950 vs (A₁'), overlap with E, 1950 vs (E, overlap with A₁'). Cr(CO)₃: 1928 m (A₁), 1905 s, 1914 s (E). Anal. Calcd for C₁₉H₁₀SO₉Cr₂: C, 44.02; H, 1.94. Found: C, 44.30; H 1.98.

[Cr(CO)₅{C(OTiCp₂Cl)((η^6 -2-BT)Cr(CO)₃)}] (**4**): yield 0.27 g, 39%. NMR (δ /ppm in C₆D₆): ¹H NMR 7.95 (d, 1H, H₃, *J* = 0.8), 5.14 (d, 1H, H₄, *J* = 6.7 Hz) 4.54 (m, 1H, H₅), 4.16 (m, 1H, H₆), 5.20 (dd, 1H, H₇, *J* = 6.7, 0.8 Hz), 5.89, 5.84 (s, s, 10H, Ti-Cp₂). IR (ν_{CO} , CH₂Cl₂, cm⁻¹): Cr(CO)₅, 2052 m (A₁'), n.o. (B), 1968 s (A₁'), 1935 vs (E, overlap with A₁ (Cr(CO)₃)); Cr(CO)₃, 1935 vs (A₁, overlap with E (Cr(CO)₅)), 1895 m (E). Anal. Calcd for C₂₇H₁₅SO₉ClCr₂Ti: C, 46.10; H, 2.15. Found: C, 46.78; H 2.37.

[Cr(CO)₅{C(OTiCp₂Cl)Fe}] (**5**): yield 0.22 g, 35%. ¹H NMR (δ , ppm, CDCl₃): 6.52 (s, 10H, Ti-Cp₂), 4.70 (br, 2H, H₃ and H₃'), 4.57 (br, 2H, H₄ and H₄'), 4.33 (s, 5H, Fe-Cp). ¹³C NMR: 306 (C1), 218 (CO_{cis}), 223 (CO_{trans}), 118, 117 (Ti-Cp₂), 110 (C2), 76 (C3, C3'), 72 (C4, C4'), 71 (Fe-Cp). IR (ν_{CO} , CH₂Cl₂, cm⁻¹): 2054 w (A₁'), 2046 vw (B), 1980 vs (A₁'), 1931 w (E). Anal. Calcd for C₂₆H₁₉O₆ClCr₂TiFe: C, 50.48; H, 3.10. Found: C, 50.71; H 3.25.

[(Cr(CO)₅)₂{ μ_2 -C₂(O₂TiCp₂-O,O')(Fe(C₅H₄)₂-C,C')}] (**6**): yield 0.18 g, 45%. ¹H NMR (δ , ppm, CDCl₃): 6.70 (s, 10H, Ti-Cp₂), 4.70 (dd, 4H, H₃, H₃', *J* = 2.0, 1.9 Hz), 4.43 (dd, 4H, H₄, H₄', *J* = 2.0, 1.9 Hz). ¹³C NMR: 313 (C1), 218 (CO_{cis}), 224 (CO_{trans}), 118 (Ti-Cp₂), n.o. (C2), 77 (C3, C3'), 72 (C4, C4'). IR (ν_{CO} , CH₂Cl₂, cm⁻¹): 2056 w (A₁'), 2044 s (B), 1979 s (A₁'), 1929 vs (E). Anal. Calcd for C₃₂H₁₈O₁₂Cr₂TiFe: C, 47.91; H, 2.26. Found: C, 48.13; H 2.32.

[(Cr(CO)₅)₂{ μ_2 -C₂(OEt)₂Fe(C₅H₄)₂-C,C')}] (**7**): yield 0.38 g, 56%. ¹H NMR (δ , ppm, CDCl₃): 5.00 (dd, 4H, H₃, H₃', *J* = 2.3, 1.9 Hz), 4.73 (dd, 4H, H₄, H₄', *J* = 2.3, 1.9 Hz), 5.07 (q, 4H, CH₂, *J* = 7.1 Hz), 1.63 (t, 6H, CH₃, *J* = 7.0 Hz). ¹³C NMR: 306 (C1), 217 (CO_{cis}), 223 (CO_{trans}), 99 (C2), 76 (C3, C3'), 73 (C4, C4'), 77 (CH₂), 15 (CH₃). IR (ν_{CO} , CH₂Cl₂, cm⁻¹): 2054 s (A₁'), 1979 sh (B), 1938 vs (A₁'), 1902 sh (E). Anal. Calcd for C₂₆H₁₈O₁₂Cr₂Fe: C, 45.77; H, 2.66. Found: C, 45.90; H 2.71.

X-ray Crystallography. The crystal data collection and refinement details for complexes **1–4** and **5–7** are summarized in Tables 4 and 5, respectively. The X-ray crystal structure analyses were performed using data collected at 293 K on a Siemens P4 diffractometer fitted with a Bruker 1K CCD detector using graphite-monochromated, Mo K α radiation by means of a combination of phi and omega scans. Data reductions were performed using SAINT+,³¹ and the intensities were corrected for absorption using SADABS.³¹ The structures were solved by direct methods using SHELXTS³¹ and refined by full-matrix least-squares using SHELXTL³¹ and SHELXL-97.³² The struc-

(31) SAINT+ Version 6.45, SADABS Version 2.10, SHELXTS and SHELXTL Version 6.14; Bruker AXS Inc.: Madison, WI, 2001.

(32) Sheldrick, G. M. SHELXL-97; University of Göttingen: Germany, 1997.

Table 4. Data Collection and Crystal Structure Details for 1–4

	1	2	3	4
formula	C ₁₆ H ₁₀ CrO ₆ S	C ₂₄ H ₁₅ ClCrO ₆ STi • CH ₂ Cl ₂	C ₁₉ H ₁₀ Cr ₂ O ₉ S	C ₂₇ H ₁₅ ClCr ₂ O ₉ STi • CH ₂ Cl ₂
fw	382.30	651.70	518.33	787.73
cryst syst	monoclinic	triclinic	triclinic	monoclinic
space group	<i>P</i> 2 ₁ / <i>m</i>	<i>P</i> $\bar{1}$	<i>P</i> $\bar{1}$	<i>P</i> 2 ₁ / <i>c</i>
cryst color	dark red	dark red	dark purple	purple
cryst dims, mm	0.40 × 0.36 × 0.09	0.42 × 0.18 × 0.14	0.22 × 0.16 × 0.05	0.28 × 0.10 × 0.015
<i>a</i> , Å	9.2928(11)	11.3041(12)	8.3523(11)	11.260(2)
<i>b</i> , Å	7.6330(9)	11.5751(12)	10.7547(15)	12.083(2)
<i>c</i> , Å	12.4413(15)	12.2429(13)	13.0118(17)	23.804(4)
α, deg		66.520(2)	109.519(2)	
β, deg	104.249(2)	88.797(2)	108.371(2)	101.009(3)
γ, deg		67.038(2)	95.519(2)	
<i>V</i> , Å ³	855.34(18)	1335.6(2)	1018.6(2)	3178.9(10)
<i>Z</i>	2	2	2	4
<i>D</i> _{calc} , g cm ^{−3}	1.484	1.620	1.690	1.646
μ, mm ^{−1}	0.818	1.123	1.219	1.285
<i>T</i> _{min} / <i>T</i> _{max}	0.751/0.929	0.664/0.855	0.795/0.941	0.690/0.981
θ range, deg	3.14–26.58	2.48–26.64	2.58–26.53	2.42–26.54
no. of reflns collected	4619	6539	5597	17 002
no. of indep reflns/ <i>R</i> (int)	1742/0.0239	4676/0.1790	3714/0.0212	6045/0.0501
<i>R</i> 1/ <i>wR</i> 2 (all data)	0.0350/0.0952	0.2111/0.3474	0.0411/0.1040	0.0946/0.1623
<i>R</i> 1/ <i>wR</i> 2 (<i>I</i> > 2σ(<i>I</i>))	0.0324/0.0912	0.1185/0.3193	0.0370/0.0992	0.0525/0.1355
params/GOF	133/1.101	334/1.242	289/1.096	447/1.054

Table 5. Data Collection and Crystal Structure Details for 5–7

	5	6	7
formula	C ₂₆ H ₁₉ ClCrFeO ₆ Ti • CH ₂ Cl ₂	C ₃₂ H ₁₈ Cr ₂ FeO ₁₂ Ti	C ₂₆ H ₁₈ Cr ₂ FeO ₁₂
fw	703.54	802.21	682.25
cryst syst	monoclinic	monoclinic	monoclinic
space group	<i>P</i> 2 ₁ / <i>n</i>	<i>P</i> 2 ₁ / <i>c</i>	<i>C</i> 2/ <i>c</i>
cryst color	red-brown	dark brown	dark red
cryst dims, mm	0.40 × 0.38 × 0.04	0.42 × 0.12 × 0.12	0.34 × 0.08 × 0.06
<i>a</i> , Å	10.2230(7)	9.9813(4)	12.3910(15)
<i>b</i> , Å	26.2984(19)	15.8650(7)	14.6211(17)
<i>c</i> , Å	10.5587(8)	20.1457(9)	14.9681(18)
β, deg	90.7190(10)	101.7230(10)	90.047(2)
<i>V</i> , Å ³	2838.5(4)	3123.6(2)	2711.8(6)
<i>Z</i>	4	4	4
<i>D</i> _{calc} , g cm ^{−3}	1.646	1.706	1.671
μ, mm ^{−1}	1.477	1.444	1.379
<i>T</i> _{min} / <i>T</i> _{max}	0.943–0.609	0.841/d 0.725	0.921/0.769
θ range, deg	2.47 to 26.38	2.43 – 26.53	2.55 to 26.43
no. of reflns collected	14 859	16 699	7163
no. of ind reflns/ <i>R</i> (int)	5143/0.0414	5958/0.0290	2537/0.0273
<i>R</i> 1/ <i>wR</i> 2 (all data)	0.0798/0.1423	0.0409/0.0911	0.0395/0.1039
<i>R</i> 1/ <i>wR</i> 2 (<i>I</i> > 2σ(<i>I</i>))	0.0488/0.1224	0.0314/0.0825	0.0360/0.0990
params/GOF	352/1.035	433/1.082	201/0.996

ture solutions and refinements for complexes **1**, **2**, **4**, **5**, and **6** were uneventful. For complex **3**, as discussed earlier, some disorder in the thienyl ring was observed with a minor orientation of the ring rotated ca. 180° with respect to the major orientation. Minor sites for S(1) and C(8)–H(8) were found and refined with constrained bond distances to neighboring atoms. Site occupation factors for the major and minor sites were refined but constrained to a sum to 1.0. The SOF for the major sites refined to 0.880(3). The crystal structure of complex **7** was refined as a two-domain merohedral twin. The domain fractional contribution refined to 0.525(2). Also for this structure the non-H atoms of the OEt group and the Cp ring bonded to the same carbene are approximately coplanar. This, together with the stacking of molecules of the complex vertically above one another in the direction parallel with the *c* axis, allows for some packing disorder in which the position of the Cp ring and the OEt group are interchanged and hence allowing minor alternative positions of the bridging ferrocenyl moiety either within the same molecule as observed for the major structural arrangement (i.e., a direct interchange between the ferrocenyl moiety and the two OEt groups) or with an effective shift of the molecule position such that the ferrocenyl moiety bridges two (CO)₅Cr-carbene moieties

which are in adjacent molecules in the major structure. Residual maxima observed in the difference map were assigned to two minor alternative positions for Fe(1), and two further maxima were assigned to minor positions for the Cp ring atoms C(10) and C(11) to complete a minor occupancy of the Cp ring at approximately the same site as that of the major OEt group; the other three Cp C atoms approximately coincide with the O and two C atoms of the OEt group. Because of the overlapping of the major and minor sites of the Cp ring and the OEt moiety, both positions of the Cp ring and of the OEt moiety were refined as rigid bodies with geometries derived from the same moieties in the structures of **1** (OEt) and **5** (Cp). To avoid refinement instability, the SOFs of the disordered moieties were refined with the ADPs of the atoms fixed. The SOFs were then fixed and the ADPs were allowed to refine.

Conclusion

In this paper we have described the first example of Fischer carbene complexes having three different transition metal fragments as substituents, and all metals are in electronic contact with the carbene carbon atom, as well as bridged

biscarbene complexes containing up to four transition metals. The potential role of the metal fragments as carbene substituents in activating or stabilizing the carbene carbon is being investigated. We are extending the range of trimetallic carbene complexes to explore the reactivity features and template effects of **4** and **5** toward small organic substrates with unsaturated bonds, as well as the redox activity of these complexes. Attention has recently been drawn to the fate of carbene ligands in reactions with one electron transfer agents and the control their carbene substituents exert on the course of reactions.⁶

Acknowledgment. The authors gratefully acknowledge the financial support provide by the National Research Foundation (NRF) to S.L. under grant number 2047221 and M.L. under grant number 2053930.

Supporting Information Available: Crystallographic data for **1–7** in CIF format have been deposited and are available free of charge via the Internet at <http://pubs.acs.org>.

OM8001735